ACS OMEGA

Open Access

http://pubs.acs.org/journal/acsodf

Article

Lipoic Acid Nanoparticles Exert Effective Antiatherosclerosis Effects through Anti-Inflammatory and Antioxidant Pathways

Xinyi Li,[▽] Mengjiao Zhang,[▽] Anni Chen, Xinqi Wang, Lan Yang, Yingjian Zhu,* and Zhaojun Li*

Cite This: *ACS Omega* 2024, 9, 48642−48649

Read Online

ACCESS | Metrics & More | Article Recommendations

ABSTRACT: Oxidative stress and inflammation are key pathological features of atherosclerotic plaques. Numerous nanomedicines have been developed to alleviate oxidative stress and reduce inflammation within plaques. However, nonbioactive carrier materials reduce the bioavailability of nanomedicines and may pose potential biological toxicity. In this study, we utilized the unique amphiphilic chemical structure of lipoic acid (LA) to prepare LA nanoparticles (LA NPs) via a self-assembly method. Leveraging the inherent anti-inflammatory and antioxidant properties of LA, these NPs were used for the treatment of atherosclerosis. In an inflammatory macrophage model, LA NPs exhibited superior anti-inflammatory activity compared to free LA. Through ultrasound imaging and pathological methods, we discovered that LA NPs demonstrated nice antiatherosclerotic effects in an atherosclerotic mice model. Immunofluorescence analysis further indicated that the antiatherosclerotic effects of LA were associated with the alleviation of oxidative stress within the plaques, reduced macrophage infiltration, and downregulation of inflammatory cytokine levels. Therefore, LA NPs offer a promising therapeutic strategy for the treatment of atherosclerosis.

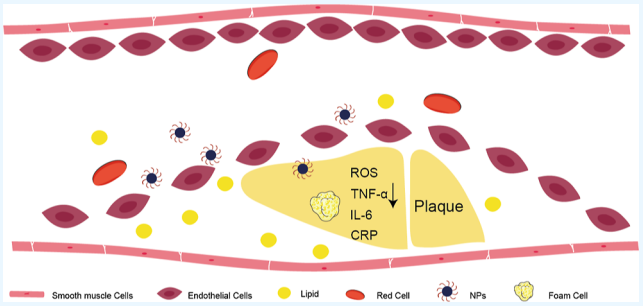

1. INTRODUCTION

Atherosclerosis is a chronic inflammatory disease characterized by the formation of atherosclerotic plaques within the vascular endothelium.[1−3] Low-density lipoprotein (LDL) within plaque is oxidized by various oxidases (such as NADPH oxidase and myeloperoxidase) and free radicals, forming oxidized LDL (ox-LDL), which is the main cause of oxidative stress.[4−6] Macrophages recognize and uptake ox-LDL through scavenger receptors on their surface to form foam cells, which ingest excessive ox-LDL, leading to apoptosis or necrosis, releasing a large amount of cellular debris and lipids, further exacerbating plaque formation and oxidative stress.[7−9] During this process, foam cells and other inflammatory cells (such as T cells and smooth muscle cells) release various inflammatory mediators (such as cytokines and chemokines), which will recruit more inflammatory cells to the vascular endothelium, intensifying the inflammatory response.[10,11] Concurrently, inhibiting inflammation and reducing oxidative stress are effective strategies for treating atherosclerosis.

Nano delivery systems have demonstrated excellent therapeutic outcomes in the field of atherosclerosis therapy due to their advantages such as efficient targeting, controlled drug release, and improved drug stability.[12,13] Recently, there have been numerous research reports on nanomedicine for the treatment of atherosclerosis.[14−19] Researchers have utilized cyclodextrin to encapsulate anti-inflammatory drugs through host−guest interactions, aiming to inhibit endoplasmic reticulum stress, enhance reendothelialization, and inhibit neointimal formation to alleviate atherosclerosis. Chai et al. developed an activatable platelet-mimicking NO nanoprodrug delivery system for the diagnosis and treatment of atherosclerosis.[20] Wang et al. constructed low molecular weight heparin derivative nanoparticles (NPs), which break the feedback regulation loop in plaque inflammation to inhibit the atherosclerosis cascade.[21,22] Despite numerous studies demonstrating the efficacy of nanomedicine in treating atherosclerosis, several challenges hinder its clinical translation. The complex chemical synthesis of carrier materials, the intricate preparation processes, the lack of biological activity of the carriers, and their potential toxic side effects remain significant obstacles.

Lipoic acid (LA) is a disulfide-containing fatty acid that functions as a coenzyme in various metabolic processes, demonstrating excellent biocompatibility.[23] LA is also a potent antioxidant that can neutralize free radicals and reduce oxidative stress, which helps in the prevention of athero-

Received: August 21, 2024
Revised: November 8, 2024
Accepted: November 19, 2024
Published: November 25, 2024

sclerosis.[24] Furthermore, LA exhibits anti-inflammatory properties, reducing the production and release of inflammatory mediators, thereby mitigating inflammation.[25−28] From a chemical perspective, LA has an amphiphilic molecular structure, which imparts it the potential for self-assembly.[29] In this study, we developed LA NPs using the ultrasonic emulsification method, which enhanced the solubility of LA without additional carrier materials, thereby improving the bioavailability. Due to the nanosize of LA NPs, they could be passively targeted to atherosclerotic plaques, increasing therapeutic efficacy. In an atherosclerotic mouse model, we confirmed that LA NPs could reduce oxidative stress and inhibit inflammation, thereby alleviating atherosclerosis. This novel approach provides a new perspective for nanotherapy in the treatment of atherosclerosis.

2. METHODS AND MATERIALS

2.1. Materials. LA (99%) was obtained from Macklin (Shanghai, China). 2′,7′-Dichlorodihydrofluorescein diacetate (DCFH-DA) was purchased from Sigma-Aldrich (USA). RAW264.7 cells were provided by the Institute of Biochemistry and Cell Biology at the Chinese Academy of Sciences (Shanghai, China). C57BL/6 male mice and apoe$^{-/-}$ male mice were purchased from the Model Animal Research Center of Nanjing University (Nanjing, China). All animal experiments were approved and performed following the guidelines of the Animal Care and Use Committee of Donghua University (approval # DHUEC-STCSM-2023−01) and also in accordance with the policy of the National Institute of Health (China). The apoe$^{-/-}$ mice were fed a high-fat diet for 4 weeks to construct the atherosclerosis model.

2.2. Preparation and Characterization of LA NPs. A 10 mg portion of LA was dissolved in 0.2 mL of dichloromethane. Subsequently, 5 mL of deionized water was added, and the mixture was subjected to ultrasonic emulsification. The resulting emulsion was then rotary evaporated to remove the dichloromethane. The obtained solution was filtered through a 0.22 μm membrane to yield LA NPs, which were then stored in an F68 solution for further use. The size and zeta potentials of LA NPs were measured by dynamic light scattering (DLS) using a Malvern Zetasizer Nano ZS90 instrument (Malvern, U.K.). The morphologies of LA NPs were observed under a transmission electron microscope (TEM, Talos F200X). The stability of NPs was assessed by detecting the variations in their size and polydispersity index (PDI) over time with the method of DLS at 4 °C and pH 7.4. The NPs were combined with 50% fetal bovine serum (FBS) and kept at 37 °C. Their transparency was then measured at a wavelength of 750 nm using a UV−visible spectrophotometer (PerkinElmer, Boston, MA) at different time points to evaluate the serum stability of NPs.

2.3. In Vitro Hemolysis Assay. 10% red blood cell (RBC) suspension was prepared from C57BL/6 mice. LA NPs with different concentrations were incubated with a RBC suspension for 1 h at 37 °C. The incubation solution was centrifuged at 3500 rpm for 5 min, and the supernatant was taken to measure the absorbance (OD) value of 540 nm with a Varioskan Flash multimode reader (Thermo, USA). Pure water was set as a positive control, and 0.9% saline was set as a negative control. The hemolysis rate was calculated according to the following formula[21]

$$\text{hemolysis}\ (\%) = (\mathrm{OD}_{\text{sample}} - \mathrm{OD}_{\text{negative}} / (\mathrm{OD}_{\text{positive}} - \mathrm{OD}_{\text{negative}})) \times 100\%$$

2.4. ROS Detection in RAW264.7 Cells. RAW264.7 cells were inoculated in 6-well plates (3×10^5 per well) and cultured at 37 °C in a 5% CO_2 atmosphere overnight. RAW264.7 cells were treated with PBS, LPS, free LA + LPS, and LA NPs + LPS (LA concentration, 10 μg/mL; LPS concentration, 500 ng/mL) for 24 h. Then the culture medium was removed, and DCFH-DA (5 μg/mL) was used to stain the cells for 1 h. The RAW264.7 cells were observed under a fluorescence microscope. According to the similar procedure, ROS generation in RAW264.7 cells were also evaluated by flow cytometry.

2.5. Secretion of Inflammatory Factors in RAW264.7 Cells. RAW264.7 cells were cultured in 24-well plates at 37 °C under a 5% CO_2 atmosphere overnight. The cells were then treated with PBS, LPS, free LA + LPS, and LA NPs + LPS (LA concentration, 10 μg/mL; LPS concentration, 500 ng/mL) for 24 h. The culture supernatant was collected, and the TNF-α, CRP, and IL-6 were measured by enzyme-linked immunosorbent assay (ELISA) (Neobioscience, China).

2.6. LA NPs Treatment on Foam Cell Formation. After incubating RAW264.7 cells in 6-well plates for 24 h and stimulating them with LPS (500 ng/mL) for another 24 h, the cells were treated with LA NPs or free LA for 4 h. Following this, ox-LDL (50 μg/mL) was added, and the cells were cultured for 48 h. The normal control group did not receive ox-LDL, while the model group was stimulated only with ox-LDL. Foam cell formation was observed under optical microscopy after staining the cells with ORO.

2.7. Animal Model Construction. Eight-week-old apoe$^{-/-}$ male mice were purchased from the Model Animal Research Center of Nanjing University. The apoe$^{-/-}$ mice were fed a high-fat diet for 4 weeks to construct the atherosclerosis model. A mouse was randomly selected and euthanized, and its aortic sinus was isolated and performed by H&E staining to verify the successful establishment of the atherosclerosis model.

2.8. In Vivo Antiatherosclerosis Assay. After the successful establishment of the atherosclerosis model, the apoe$^{-/-}$ male mice were randomly divided into 3 groups (n = 6), and the treatment was started on the fifth week after the high-fat diet. The mice were intravenously injected with saline, free LA, and LA NPs (at an equivalent dose of 5 mg/kg LA. w/w). Each formulation was administered twice a week for 8 weeks. C57BL/6 mice with a normal diet acted as a negative control group. After treatment, the aortic arch and abdominal aorta were examined by ultrasound imaging. Then, the mice were euthanized, and their aortas were separated, opened longitudinally, and stained with ORO. Sections of the aorta were also prepared and stained with ORO. For the immunohistochemistry study, sections of aortic tissue were incubated with antibodies to CD68, ROS, and IL-6. In addition, serum was collected for blood lipid analysis.

2.9. In Vivo Toxicology Evaluations. At the end of treatment, whole blood from the mice was obtained in anticoagulative tubes, and the serum was collected for liver and kidney function analysis. Their major organs (liver, spleen, and kidney) were isolated, and the histological sections were prepared and stained with H&E to evaluate the toxicity of NPs.

https://doi.org/10.1021/acsomega.4c07745
ACS Omega 2024, 9, 48642−48649

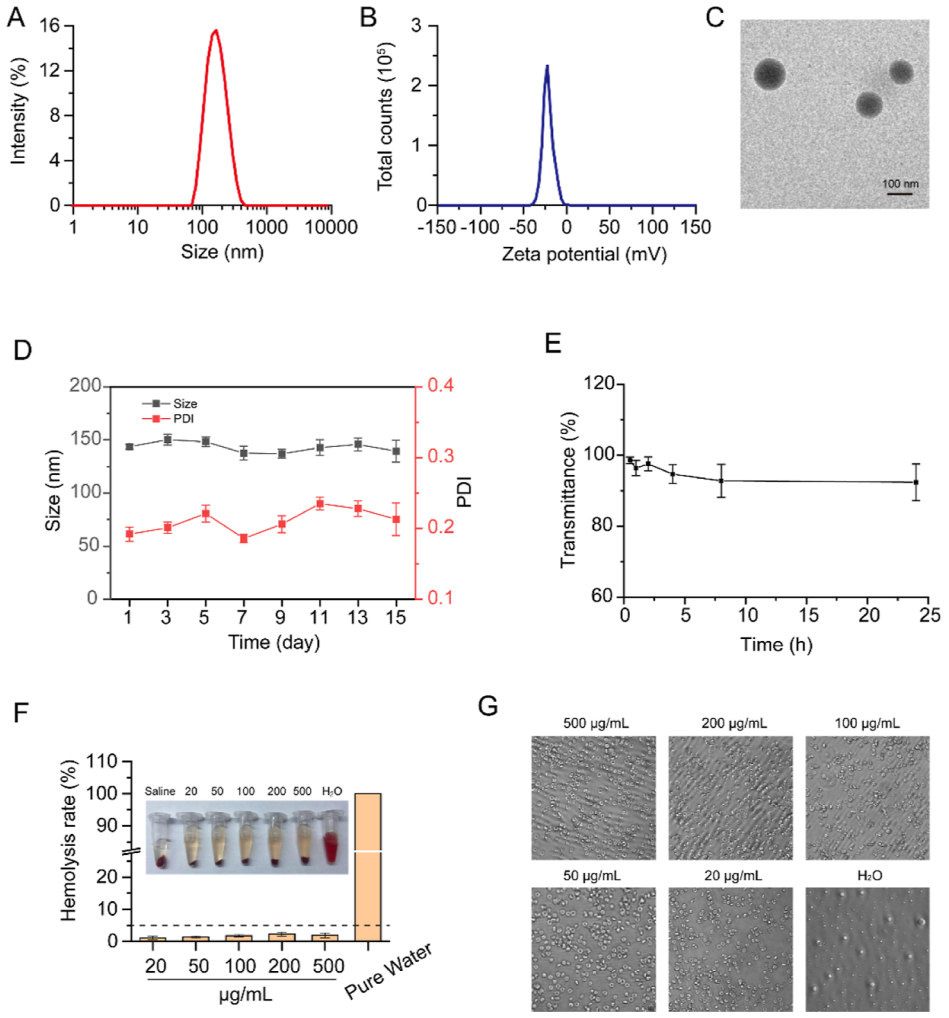

Figure 1. Characterization of LA NPs and evaluation of its hemolysis. (A,B) Size distribution and zeta potential of LA NPs. (C) TEM of LA NPs. (D) Stability of LA NPs over a 15 day period at 4 °C and pH 7.4 condition. Mean ± SD, $n = 3$. (E) Transmittance vs time curve of LA NPs after incubation with 50% FBS. Mean ± SD, $n = 3$. (F) Hemolysis rate of LA NPs, with an embedded hemolysis image. (G) Morphological image of red blood cells.

2.10. Statistical Analysis. Data was reported as the mean ± SD. All statistical analyses were performed using SPSS version 21.0 (SPSS Inc., Chicago, IL, USA). The experimental data were statistically analyzed by using the *t*-test between two independent samples. A *p*-value <0.05 was considered significantly different. *P* values less than 0.05, 0.01, 0.001, and 0.0001 were denoted by *, **, ***, and ****, respectively.

3. RESULTS AND DISCUSSION

3.1. Characterization of LA NPs and Their Blood Compatibility. Due to the amphiphilic nature of LA, which features both hydrophilic carboxyl groups and hydrophobic hydrocarbon chains in its molecular structure, it can form into NPs by the self-assembling method. As shown in Figure 1A−C, DLS measurements show that the LA NPs have a diameter of approximately 140 nm, a PDI of about 0.2, and a zeta potential of 20 mV (Figure 1A,B). TEM shows that the morphology of LA NPs is spherical and the particle size is consistent with the results obtained from DLS (Figure 1C). The storage stability of LA NPs at pH 7.4 and 4 °C was evaluated by tracking changes in NP size and PDI. No significant changes were observed in either parameter over a two-week period, indicating good storage stability (Figure 1D). Additionally, the stability of the NPs in serum was tested by incubating them with 50% FBS at 37 °C. No notable changes in transmission were detected over 24 h, confirming that the LA NPs remained stable in 50% FBS (Figure 1E). The blood compatibility of NPs is an important parameter that needs to be evaluated for clinical use. As shown in Figure 1F, despite a concentration of 0.5 mg/mL, LA NPs did not cause hemolysis, and their hemolysis rate remained below 5%. Additionally, the morphology of RBCs remained normal after coincubation with LA NPs, demonstrating their good blood compatibility (Figure 1G). The above results show that LA NPs have appropriate size and blood compatibility, laying the material foundation for further research.

3.2. Anti-Inflammatory and Antioxidant Properties of LA NPs. Oxidative stress exists in the atherosclerotic plaque microenvironment, and there are a large number of inflammatory factors infiltrating. Reducing oxidative stress and anti-inflammatory are effective treatment strategies for arteriosclerosis.[30] Therefore, we used LPS-induced RAW264.7 cells as an inflammatory cell model to evaluate the anti-inflammatory and antioxidant effects of LA NPs. As shown in Figure 2A, with LPS stimulation, the RAW264.7 exhibits

https://doi.org/10.1021/acsomega.4c07745
ACS Omega 2024, 9, 48642−48649

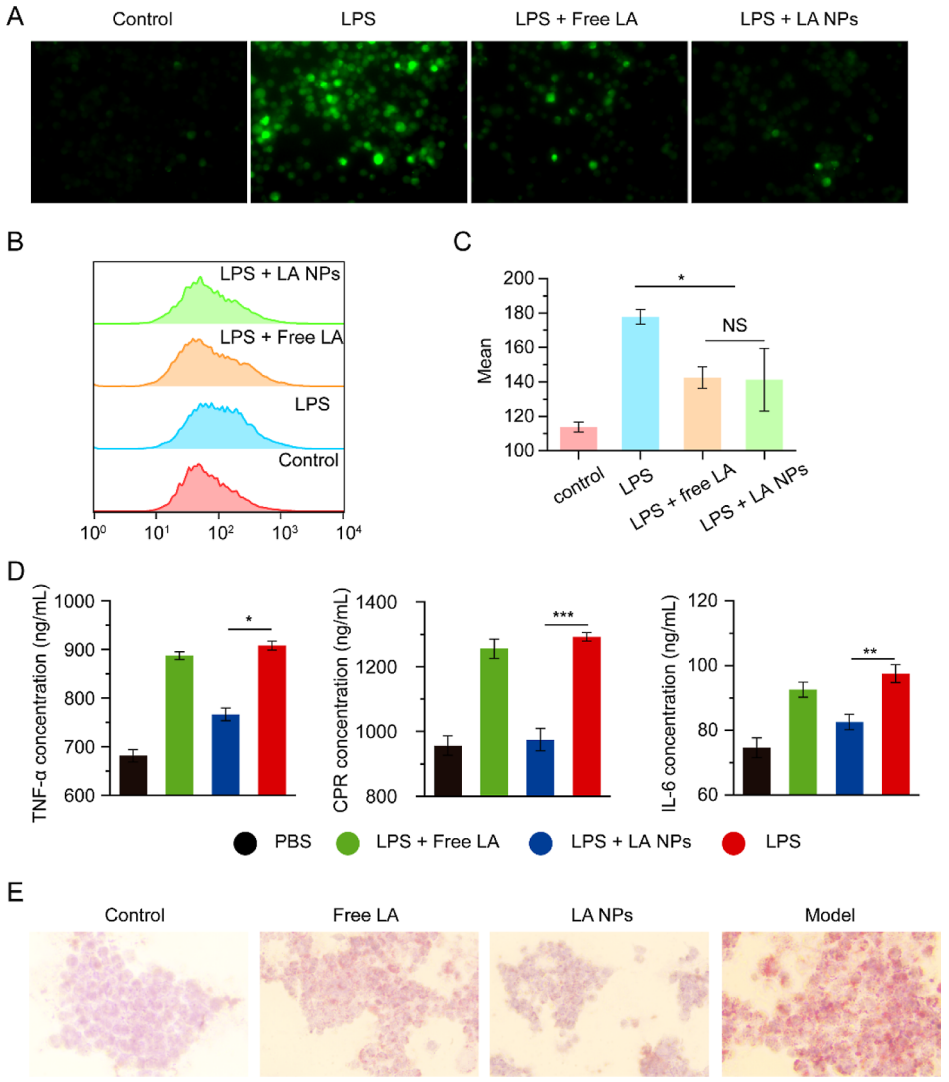

Figure 2. In vitro anti-inflammatory evaluation of NPs. (A) Fluorescent imaging of ROS production in LPS-stimulated RAW264.7 cells labeled with DCFH-DA (scale bar = 10 μm). (B, C) Flow cytometry quantification of intracellular ROS levels in RAW264.7 cells subjected to various treatments. Mean ± SD, $n = 3$. *$P < 0.05$. (D) Inflammatory cytokines TNF-α, IL-6, and CRP released by RAW264.7 cells following treatment with different formulations. Mean ± SD, $n = 3$. *$P < 0.05$, **$p < 0.01$, ***$p < 0.001$. (E) Representative ORO stained RAW264.7 cells treated with different groups.

strong green fluorescence, indicating severe oxidative stress within the cells. After free LA or LA NPs treatment, the intensity of green fluorescence decreased, indicating the good antioxidant effects of LA. The quantitative results from the flow cytometer also showed that both free LA and LA NPs can reduce oxidative stress (Figure 2B,C). Moreover, representative inflammatory factors, such as TNF-α, CPR, and IL-6, were detected by the ELISA method, and the result is shown in Figure 2D. After LPS treatment, the levels of TNF-α, CPR, and IL-6, were up-regulated. However, LA NPs could inhibit the upregulation of these inflammatory factors. Free LA could not inhibit the upregulation, probably due to low solubility. The above results indicated that LA NPs have anti-inflammatory and antioxidant properties. In addition, foam cell formation was the key index of atherosclerosis development. Thus, foam cell formation in macrophages treated with LA NPs was evaluated, as shown in Figure 2E. Both free LA and LA NPs could obviously inhibit foam cell formation compared with the model group. LA NPs showed slightly better effect than free LA, which provided direct evidence of foam cell formation suppression.

3.3. Establishment of Atherosclerosis Model of apoe$^{-/-}$ Mice and Ultrasound Imaging. Given the good anti-inflammatory and antioxidant effects of NPs, we further investigated their efficacy in vivo, and the treatment regimen timeline is shown in Figure 3A. First, the apoe$^{-/-}$ mice were fed with high fat for one month to establish a mice model of atherosclerosis. One mouse was selected, and its aortic sinus was isolated for H&E staining, and the results are shown in Figure 3B. There was significant intimal hyperplasia and foam cell deposition in the aortic sinus vessels of mice, indicating successful establishment of an atherosclerosis model. After a two-month treatment, the aortic arch and abdominal aorta were observed by ultrasound imaging to determine the therapy effect. As shown in Figure 3C, ultrasound images of mice in the saline group showed significant bulges at the bend of the aortic arch and significant thickening of the abdominal aortic vessel wall, both of which represent the progression of atherosclerotic plaque. There was also obvious thickening shown by

https://doi.org/10.1021/acsomega.4c07745
ACS Omega 2024, 9, 48642−48649

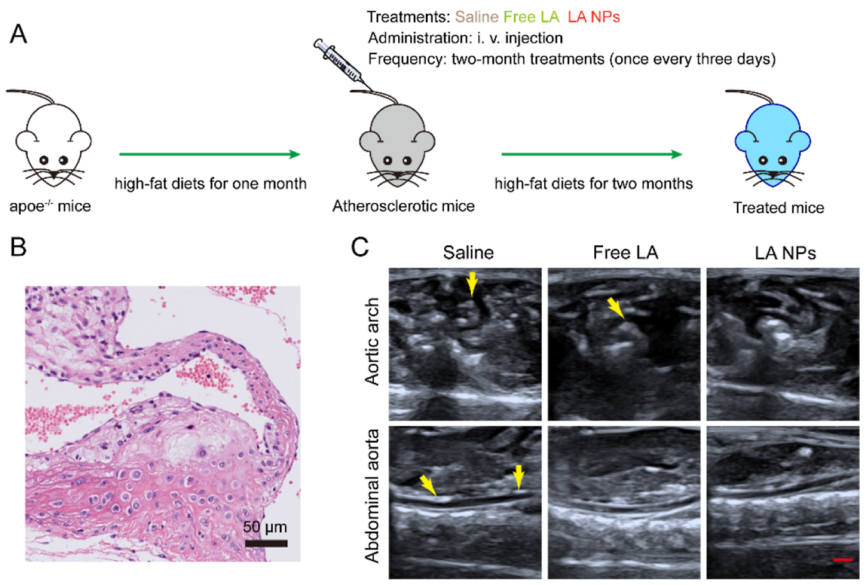

Figure 3. (A) Treatment regimen timeline for combating arteriosclerosis. (B) H&E staining image of the aortic sinus in apoe$^{-/-}$ mice with atherosclerosis. (C) Ultrasound images of abdominal aorta and aortic arch in atherosclerosis mice after treatment.

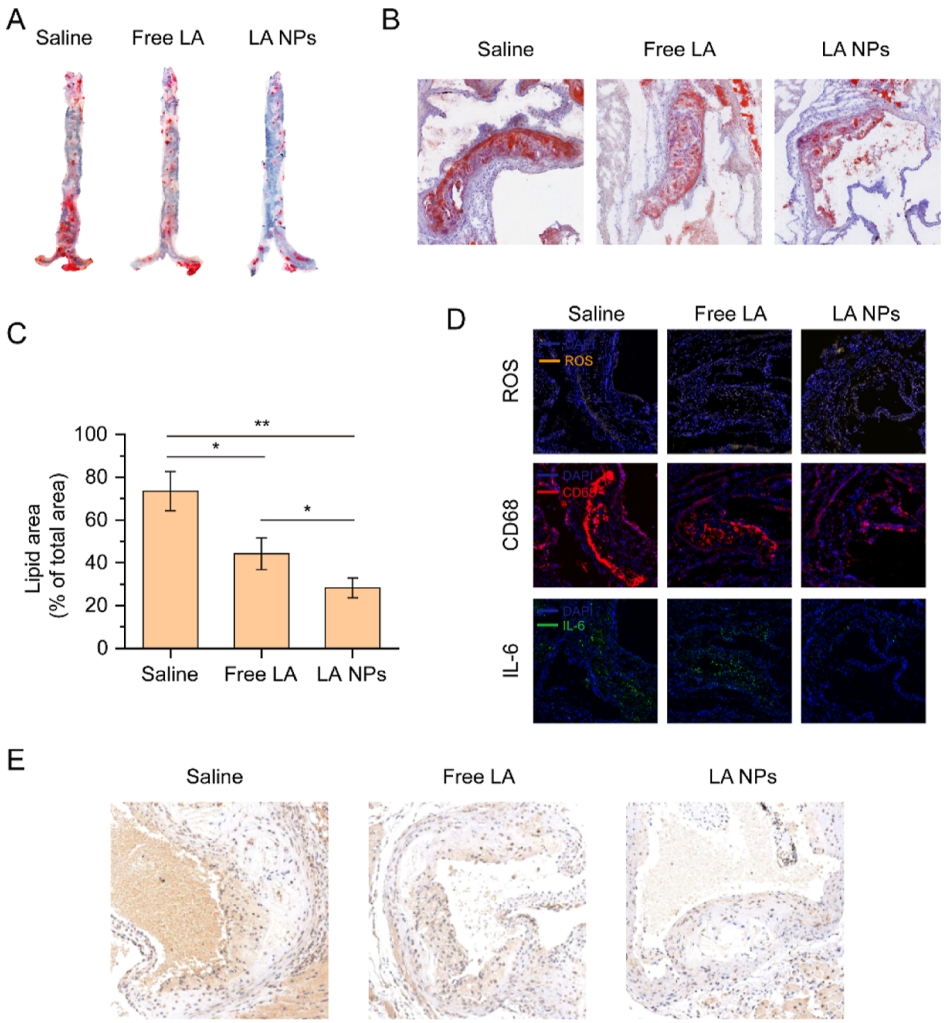

Figure 4. Evaluation of the treatment efficacy of LA NPs on atherosclerotic plaque. (A) Image of ORO-stained en face aortas. (B) Representative images of aortic sinus sections stained with ORO. (C) Quantitative analysis of plaque content in aortic sinus sections stained with ORO. Mean ± SD, $n = 3$, *$p < 0.05$, **$p < 0.01$. (D) Sections of aortic sinus stained with DHE staining, antibody to CD68, and IL-6. (E) Sections of aortic sinus stained with antibody to NF-κB.

https://doi.org/10.1021/acsomega.4c07745
ACS Omega 2024, 9, 48642−48649

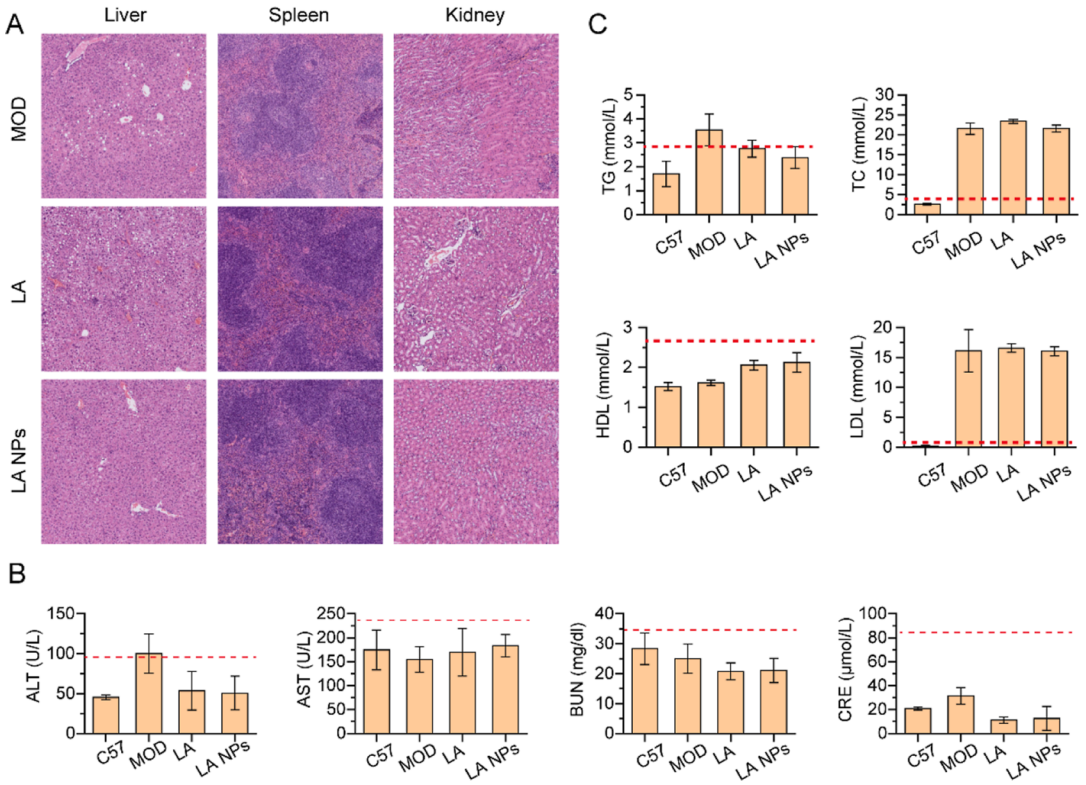

Figure 5. Histopathological examination and serum evaluation. (A) H&E staining of heart, liver, spleen, lung, and kidney. (B) Serum levels of TG, TC, HDL, and LDL. Mean ± SD, n = 3. (C) Levels of ALT, AST, BUN, and CRE after treatment in apoe$^{-/-}$ mice. Mean ± SD, n = 3.

ultrasound images of mice in the free LA group. However, there was no obvious hyperplasia of the abdominal aorta in mice of LA NPs group, and its aortic arch was smooth, which showed good antiatherosclerosis effect of LA NPs.

3.4. Pathological Evaluation of Antiatherosclerosis. After the treatment was completed, the mice were sacrificed, their aortas were isolated, and oil red O staining was performed. Representative oil red O staining of the aorta is shown in Figure 4A. It was evident that the aortas of mice in the saline group, which did not receive treatment, exhibited extensive oil red O positive areas, indicating rapid progression of atherosclerosis. According to the oil red positive area, both free LA and LA NPs exhibited antiatherosclerotic effects, with LA NPs showing a stronger effect compared to free LA. Moreover, oil red O staining of aortic sinus sections further demonstrated the significant antiatherosclerotic effects of LA NPs, as evidenced by the inhibition of lipid infiltration within the plaques (Figure 4B,C). To further elucidate the mechanism of antiatherosclerosis by LA NPs, we conducted an additional study on the oxidative stress and inflammatory environment within the plaques. The immunofluorescence results are shown in Figure 4D. ROS and IL-6 were up-regulated, and the macrophage content significantly increased within the plaques, indicating that inflammation and oxidative stress are risk factors of atherosclerosis. After treatment with free LA and LA NPs, the levels of ROS and IL-6 decreased and macrophage infiltration was reduced. Moreover, we found that the anti-inflammatory effect of the NPs is related to inhibition of the NF-κB pathway. LA NPs obviously reduced NF-κB expression within the plaque. Compared with free LA, LA NPs showed better therapeutic efficacy owing to better anti-inflammatory and antioxidant effects.

3.5. Biosafety Evaluation of NPs. Biosafety is a prerequisite for the clinical use of nanomedicine. Liver, spleen, and kidney were sliced and stained with H&E to evaluate the biosafety of the NPs. Except for mild symptoms of a fatty liver, no morphological damage was observed in other organs (Figure 5A). Besides, the liver and kidney function indicators of mice in all groups were normal (Figure 5B). All these results show that the NPs have good biosafety. Further, we investigated the blood lipid levels of each group of mice. The blood lipid levels of atherosclerotic mice were all high, and there was no significant difference between treatment groups, suggesting that the antiatherosclerosis mechanism of LA NPs has nothing to do with lowering blood lipid (Figure 5C).

4. CONCLUSIONS

In summary, based on the amphiphilic chemical structure of LA, we prepared uniformly sized LA NPs using a self-assembly method. By constructing a macrophage inflammation model, we confirmed the inherent antioxidant and anti-inflammatory properties of LA. Furthermore, we used apoe$^{-/-}$ mice to establish an atherosclerosis model and evaluated the antiatherosclerotic efficacy of LA NPs through ultrasound imaging and pathological methods. We elucidated that their good efficacy was related to their anti-inflammatory and oxidative stress-reducing properties. Additionally, we assessed the biosafety of LA NPs, suggesting that they are promising nanodrugs with antiatherosclerotic properties.

AUTHOR INFORMATION

Corresponding Authors

Zhaojun Li − *Department of Ultrasound, Jiading Branch of Shanghai General Hospital, Shanghai Jiao Tong University*

https://doi.org/10.1021/acsomega.4c07745
ACS Omega 2024, 9, 48642−48649

School of Medicine, Shanghai 201803, China; Department of Ultrasound, Shanghai General Hospital, Shanghai Jiao Tong University School of Medicine, Shanghai 200080, China; orcid.org/0000-0001-6459-3667; Email: lzj_1975@sina.com

Yingjian Zhu − *Department of Urology, Jiading Branch of Shanghai General Hospital, Shanghai Jiao Tong University School of Medicine, Shanghai 201803, China;* Email: zhuyingjian_sjtu@126.com

Authors

Xinyi Li − *Department of Ultrasound, Jiading Branch of Shanghai General Hospital, Shanghai Jiao Tong University School of Medicine, Shanghai 201803, China; School of Life Sciences, Hubei University, Wuhan, Hubei 430061, China*

Mengjiao Zhang − *Department of Ultrasound, Shanghai General Hospital, Shanghai Jiao Tong University School of Medicine, Shanghai 200080, China; School of Medical Imaging, Shandong Second Medical University, Weifang, Shandong 261053, China*

Anni Chen − *Department of Ultrasound, Shanghai General Hospital, Shanghai Jiao Tong University School of Medicine, Shanghai 200080, China; School of Medical Imaging, Shandong Second Medical University, Weifang, Shandong 261053, China*

Xinqi Wang − *Department of Ultrasound, Shanghai General Hospital, Shanghai Jiao Tong University School of Medicine, Shanghai 200080, China; Medical Imaging Technology, First Clinical College, Fujian University of Traditional Chinese Medicine, Fuzhou 350108, China*

Lan Yang − *Department of Ultrasound, Shanghai General Hospital, Shanghai Jiao Tong University School of Medicine, Shanghai 200080, China; College of Laboratory, Chengdu Medical College, Chengdu, Sichuan 610083, China*

Complete contact information is available at: https://pubs.acs.org/10.1021/acsomega.4c07745

Author Contributions

[▽]Xinyi Li and Mengjiao Zhang have contributed equally to this work. Xinyi Li and Mengjiao Zhang wrote the main manuscript text and finished almost experiments. Anni Chen, Xinqi Wang, and Lan Yang made substantial contributions to interpretation of data. Yingjian Zhu and Zhaojun Li guided the entire research, revised manuscript, and provided funding. All authors reviewed the manuscript.

Notes

The authors declare no competing financial interest.

■ ACKNOWLEDGMENTS

This work was supported by the Shanghai Health and Family Planning Commission Fund (202240235), the Natural Science Foundation of Shanghai (21ZR1451400), and the Shanghai Jiading District Health and Family Planning Commission Fund (2021-KY-10, 2021-KY-09).

■ REFERENCES

(1) Libby, P.; Ridker, P. M.; Maseri, A. Inflammation and Atherosclerosis. *Circulation* **2002**, *105* (9), 1135−1143.

(2) Kobiyama, K.; Ley, K. Atherosclerosis. *Circ. Res.* **2018**, *123* (10), 1118−1120.

(3) Shishehbor, M. H.; Bhatt, D. L. Inflammation and atherosclerosis. *Curr. Atheroscler. Rep.* **2004**, *6* (2), 131−139.

(4) Marrero, N.; Jha, K.; Razavi, A. C.; Boakye, E.; Anchouche, K.; Dzaye, O.; Budoff, M. J.; Tsai, M. Y.; Shah, S. J.; Rotter, J. I.; Guo, X.; Yao, J.; Blumenthal, R. S.; Thanassoulis, G.; Post, W. S.; Blaha, M. J.; Whelton, S. P. Identifying People at High Risk for Severe Aortic Stenosis: Aortic Valve Calcium Versus Lipoprotein(a) and Low-Density Lipoprotein Cholesterol. *Circulation: Cardiovas. Imag.* **2024**, *17* (6), No. e016372.

(5) Harrison, D.; Griendling, K. K.; Landmesser, U.; Hornig, B.; Drexler, H. Role of oxidative stress in atherosclerosis. *Am. J. Cardiol.* **2003**, *91* (3), 7−11.

(6) Poznyak, A. V.; Grechko, A. V.; Orekhova, V. A.; Chegodaev, Y. S.; Wu, W.-K.; Orekhov, A. N. Oxidative Stress and Antioxidants in Atherosclerosis Development and Treatment. *Biology* **2020**, *9*, 60.

(7) Ji, M.; Wei, Y.; Ye, Z.; Hong, X.; Yu, X.; Du, R.; Li, Q.; Sun, W.; Liu, D. In Vivo Fluorescent Labeling of Foam Cell-Derived Extracellular Vesicles as Circulating Biomarkers for In Vitro Detection of Atherosclerosis. *J. Am. Chem. Soc.* **2024**, *146* (14), 10093−10102.

(8) Akther, F.; Sajin, D.; Moonshi, S. S.; Wu, Y.; Vazquez-Prada, K. X.; Ta, H. T. Modeling Foam Cell Formation in A Hydrogel-Based 3D-Intimal Model: A Study of The Role of Multi-Diseases During Early Atherosclerosis. *Adv. Biol.* **2024**, *8* (4), 2300463.

(9) Ma, C.; Li, Y.; Tian, M.; Deng, Q.; Qin, X.; Lu, H.; Gao, J.; Chen, M.; Weinstein, L. S.; Zhang, M.; Bu, P.; Yang, J.; Zhang, Y.; Zhang, C.; Zhang, W. Gsα Regulates Macrophage Foam Cell Formation During Atherosclerosis. *Circ. Res.* **2024**, *134* (7), e34−e51.

(10) Fredman, G.; Serhan, C. N. Specialized pro-resolving mediators in vascular inflammation and atherosclerotic cardiovascular disease. *Nat. Rev. Cardiol.* **2024**, *21*, 808.

(11) Döring, Y.; van der Vorst, E. P. C.; Weber, C. Targeting immune cell recruitment in atherosclerosis. *Nat. Rev. Cardiol.* **2024**, *21*, 824.

(12) Wang, S.; He, H.; Mao, Y.; Zhang, Y.; Gu, N. Advances in Atherosclerosis Theranostics Harnessing Iron Oxide-Based Nanoparticles. *Advanced Science* **2024**, *11* (17), 2308298.

(13) Liu, Y.; Jiang, Z.; Yang, X.; Wang, Y.; Yang, B.; Fu, Q. Engineering Nanoplatforms for Theranostics of Atherosclerotic Plaques. *Adv. Healthcare Mater.* **2024**, *13* (16), 2303612.

(14) He, Z.; Chen, W.; Hu, K.; Luo, Y.; Zeng, W.; He, X.; Li, T.; Ouyang, J.; Li, Y.; Xie, L.; Zhang, Y.; Xu, Q.; Yang, S.; Guo, M.; Zou, W.; Li, Y.; Huang, L.; Chen, L.; Zhang, X.; Saiding, Q.; Wang, R.; Zhang, M.-R.; Kong, N.; Xie, T.; Song, X.; Tao, W. Resolvin D1 delivery to lesional macrophages using antioxidative black phosphorus nanosheets for atherosclerosis treatment. *Nat. Nanotechnol.* **2024**, *19*, 1386−1398.

(15) Fu, C.; Tao, Y.; Li, Z.; Yao, Y.; Lin, F.; He, D.; Chen, H.; Ma, J.; Xiao, Y.; Liu, L.; Liang, X.-J.; Guo, W. Circulating monocyte differentiation-activated nanoprodrugs for reprogramming macrophage immunity in atherosclerotic plaques. *Nano Today* **2024**, *56*, 102304.

(16) Li, Z.; Wang, Q.; Jing, H.; Luo, X.; Du, L.; Duan, Y. cRGD Peptide-Modified Nanocarriers for Targeted Delivery of Angiogenesis Inhibitors to Attenuate Advanced Atherosclerosis. *ACS Appl. Nano Mater.* **2021**, *4* (11), 11554−11562.

(17) Chen, W.; Schilperoort, M.; Cao, Y.; Shi, J.; Tabas, I.; Tao, W. Macrophage-targeted nanomedicine for the diagnosis and treatment of atherosclerosis. *Nat. Rev. Cardiol.* **2022**, *19* (4), 228−249.

(18) Cheng, J.; Huang, H.; Chen, Y.; Wu, R. Nanomedicine for Diagnosis and Treatment of Atherosclerosis. *Advanced Science* **2023**, *10* (36), 2304294.

(19) Lobatto, M. E.; Fuster, V.; Fayad, Z. A.; Mulder, W. J. M. Perspectives and opportunities for nanomedicine in the management of atherosclerosis. *Nat. Rev. Drug Discovery* **2011**, *10* (11), 835−852.

(20) Chai, Y.; Shangguan, L.; Yu, H.; Sun, Y.; Huang, X.; Zhu, Y.; Wang, H.-Y.; Liu, Y. Near Infrared Light-Activatable Platelet-Mimicking NIR-II NO Nano-Prodrug for Precise Atherosclerosis Theranostics. *Advanced Science* **2024**, *11* (3), 2304994.

(21) Wang, Q.; Duan, Y.; Jing, H.; Wu, Z.; Tian, Y.; Gong, K.; Guo, Q.; Zhang, J.; Sun, Y.; Li, Z.; Duan, Y. Inhibition of atherosclerosis

progression by modular micelles. *J. Controlled Release* **2023**, *354*, 294−304.
(22) Wang, Q.; Jing, H.; Lin, J.; Wu, Z.; Tian, Y.; Gong, K.; Guo, Q.; Yang, X.; Wang, L.; Li, Z.; Duan, Y. Programmed prodrug breaking the feedback regulation of P-selectin in plaque inflammation for atherosclerotic therapy. *Biomaterials* **2022**, *288*, 121705.
(23) Gorąca, A.; Huk-Kolega, H.; Piechota, A.; Kleniewska, P.; Ciejka, E.; Skibska, B. Lipoic acid − biological activity and therapeutic potential. *Pharmacol. Rep.* **2011**, *63* (4), 849−858.
(24) Wollin, S. D.; Jones, P. J. H. α-Lipoic Acid and Cardiovascular Disease. *J. Nutr.* **2003**, *133* (11), 3327−3330.
(25) Salehi, B.; Berkay Yılmaz, Y.; Antika, G.; Boyunegmez Tumer, T.; Fawzi Mahomoodally, M.; Lobine, D.; Akram, M.; Riaz, M.; Capanoglu, E.; Sharopov, F.; Martins, N.; Cho, W. C.; Sharifi-Rad, J. Insights on the Use of α-Lipoic Acid for Therapeutic Purposes. *Biomolecules* **2019**, *9*, 356.
(26) Tibullo, D.; Li Volti, G.; Giallongo, C.; Grasso, S.; Tomassoni, D.; Anfuso, C. D.; Lupo, G.; Amenta, F.; Avola, R.; Bramanti, V. Biochemical and clinical relevance of alpha lipoic acid: antioxidant and anti-inflammatory activity, molecular pathways and therapeutic potential. *Inflammation Res.* **2017**, *66* (11), 947−959.
(27) Salinthone, S.; Yadav, V.; Schillace, R. V.; Bourdette, D. N.; Carr, D. W. Lipoic Acid Attenuates Inflammation via cAMP and Protein Kinase A Signaling. *PLoS One* **2010**, *5* (9), No. e13058.
(28) Maczurek, A.; Hager, K.; Kenklies, M.; Sharman, M.; Martins, R.; Engel, J.; Carlson, D. A.; Münch, G. Lipoic acid as an anti-inflammatory and neuroprotective treatment for Alzheimer's disease. *Adv. Drug Delivery Rev.* **2008**, *60* (13−14), 1463−1470.
(29) Nishiura, H. A Novel Nano-Capsule of α-Lipoic Acid as a Template of Core-Shell Structure Constructed by Self-Assembly. *J. Nanomed. Nanotechnol.* **2013**, *04* (01), 1000155.
(30) Marchio, P.; Guerra-Ojeda, S.; Vila, J. M.; Aldasoro, M.; Victor, V. M.; Mauricio, M. D. Targeting Early Atherosclerosis: A Focus on Oxidative Stress and Inflammation. *Oxid. Med. Cell. Longevity* **2019**, *2019* (1), 8563845.

https://doi.org/10.1021/acsomega.4c07745
ACS Omega 2024, 9, 48642−48649